A Many-Objective Test Problem for Visually Examining Diversity Maintenance Behavior in a Decision Space

Hisao Ishibuchi
Graduate School of Engineering
Osaka Prefecture University
Sakai, Osaka 599-8531, Japan
+81-72-254-9350
hisaoi@cs.osakafu-u.ac.jp

Naoya Akedo
Graduate School of Engineering
Osaka Prefecture University
Sakai, Osaka 599-8531, Japan
+81-72-254-9198
naoya.akedo@ci.cs.osakafu-u.ac.jp

Yusuke Nojima
Graduate School of Engineering
Osaka Prefecture University
Sakai, Osaka 599-8531, Japan
+81-72-254-9198
nojima@cs.osakafu-u.ac.jp

ABSTRACT
Recently distance minimization problems in a two-dimensional decision space have been utilized as many-objective test problems to visually examine the behavior of evolutionary multi-objective optimization (EMO) algorithms. Such a test problem is usually defined by a single polygon where the distance from a solution to each vertex is minimized in the decision space. We can easily generate different test problems from different polygons. We can also easily generate test problems with multiple equivalent Pareto optimal regions using multiple polygons of the same shape and the same size. Whereas these test problems have a number of advantages, they have no clear relevance to real-world situations since they are artificially generated unrealistic test problems. In this paper, we generate a distance minimization problem from a real-world map. Our test problem has four objectives, which are to minimize the distances to the nearest elementary school, junior high school, railway station, and convenience store. Using our test problem, we examine the behavior of well-known and frequently-used EMO algorithms in terms of their diversity maintenance ability in the two-dimensional decision space.

Categories and Subject Descriptors
I.2.8 [**Artificial Intelligence**]: Problem Solving, Control Methods, and Search – *Heuristic Methods.*

General Terms
Algorithms.

Keywords
Evolutionary multiobjective optimization (EMO), many-objective optimization problems, decision space diversity.

1. INTRODUCTION
Many-objective optimization is a hot issue in the research field of evolutionary multi-objective optimization (EMO). This is because well-known EMO algorithms such as NSGA-II [6] and SPEA [25] do not work well on multi-objective problems with four or more objectives. Whereas a large number of EMO algorithms have been proposed in the literature [3]-[5], [18], most algorithms can be characterized by the following three common features: Pareto dominance-based fitness evaluation, diversity maintenance, and elitism. Those EMO algorithms do not work well on many-objective problems since almost all solutions in the current population become non-dominated with each other under many objectives. That is, Pareto dominance-based fitness evaluation cannot generate strong selection pressure toward the Pareto front as pointed out by many studies [8], [10], [11], [14].

In the implementation of an EMO algorithm (also evolutionary algorithms in general), the point is to find a good balance between convergence improvement and diversity maintenance. When an EMO algorithm is applied to a two-objective problem, we can visually examine the convergence-diversity balance by depicting all solutions in each generation in the two-dimensional objective space. Such a visual examination of the EMO algorithm in the objective space is of great help in its appropriate implementation. However, it is very difficult to visually examine the behavior of the EMO algorithm in the objective space when it is applied to a many-objective problem.

Recently distance minimization problems in a two-dimensional decision space have been used as many-objective test problems to visually examine the behavior of EMO algorithms [12], [17]. Such a test problem is defined by a single polygon where the distance from a solution to each vertex is minimized in the decision space. Thus the number of objectives is equal to the number of vertices of the polygon. So we can easily generate test problems with an arbitrary number of objectives. All points in the polygon (including points on the sides) are Pareto optimal solutions. Such a test problem in a two-dimensional decision space can be generalized as many-objective problems in a high-dimensional decision space [16]. By using multiple polygons with the same size and the same shape, we can also generate many-objective problems with multiple equivalent Pareto regions [9], [15]. Test problems with multiple equivalent Pareto regions are used to examine decision space diversity of obtained non-dominated solutions by EMO algorithms. Diversity maintenance in EMO algorithms has been mainly discussed in the objective space in order to find uniformly distributed non-dominated solutions along the Pareto front. However, some recent studies discussed decision space diversity to search for a variety of non-dominated solutions in the decision space [13], [15], [19].

GECCO'11, July 12–16, 2011, Dublin, Ireland.

Whereas distance minimization problems have a lot of advantages as many-objective test problems, they have no clear relevance to real-world situations. They are artificially generated unrealistic test problems. As a result, such a test problem cannot show the importance of decision space diversity in an understandable manner. In this paper, we generate a distance minimization problem from a real-world map (instead of polygons). Our test problem has four objectives, which are related to four different types of facilities in the map: elementary schools, junior high schools, railway stations, and convenience stores. Each objective is defined by the distance to the nearest facility in each group. Using our test problem, we examine the behavior of well-known and frequently-used EMO algorithms: NSGA-II [6], SPEA2 [24], MOEA/D [21], and SMS-EMOA [2]. NSGA-II and SPEA2 are standard Pareto dominance-based EMO algorithms. MOEA/D is a scalarizing function-based EMO algorithm while SMS-EMOA is an indicator-based EMO algorithm. These two algorithms do not use Pareto dominance-based fitness evaluation schemes.

This paper is organized as follows. First, we briefly explain multi-objective distance minimization problems in a two-dimensional decision space in Section 2. Next, we show our test problem generated from a real-world map in Section 3. Then, we examine the behavior of NSGA-II, SPEA2, MOEA/D and SMS-EMOA in Section 4 through computational experiments on some distance minimization problems with polygons and our test problem. The focus of our study is placed on decision space diversity of obtained non-dominated solutions by each algorithm. It is shown that each algorithm has different behaviors between polygon-based and map-based test problems. It is also shown that intuitive evaluation of decision space diversity is somewhat different from hypervolume-based evaluation of solution sets in the objective space. Finally, we conclude this paper in Section 5.

2. POLYGON-BASED TEST PROBLEMS

In this section, we explain distance minimization problems with multiple polygons. Let us assume that we have m polygons with k vertices. These polygons can be different in their shape and size whereas we first explain test problems with multiple polygons of the same size and the same shape. We denote the vertices of the jth polygon by A_j, B_j, ... (j = 1, 2, ..., m) as shown in Fig. 1. The number of objectives is the same as the number of vertices (i.e., k). For example, Fig. 1 shows a three-objective test problem defined by four triangles of the same size and the same shape.

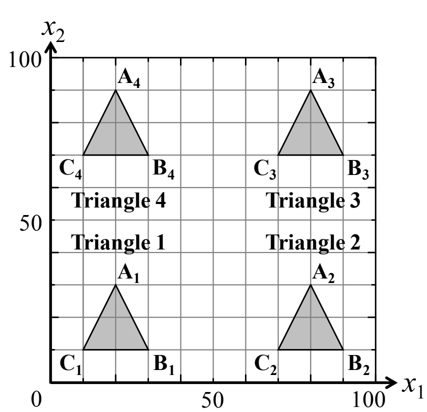

Figure 1. A polygon-based three-objective test problem.

The ith objective to be minimized is the distance from a solution to the nearest ith vertex over the given m polygons. For example, the three-objective test problem in Fig. 1 (m = 4) is written as

$$f_1(\mathbf{x}) = \min \{d(\mathbf{x}, A_1), d(\mathbf{x}, A_2), d(\mathbf{x}, A_3), d(\mathbf{x}, A_4)\}, \quad (1)$$

$$f_2(\mathbf{x}) = \min \{d(\mathbf{x}, B_1), d(\mathbf{x}, B_2), d(\mathbf{x}, B_3), d(\mathbf{x}, B_4)\}, \quad (2)$$

$$f_3(\mathbf{x}) = \min \{d(\mathbf{x}, C_1), d(\mathbf{x}, C_2), d(\mathbf{x}, C_3), d(\mathbf{x}, C_4)\}, \quad (3)$$

where $\mathbf{x}$ is a solution in the two-dimensional decision space (i.e., $\mathbf{x} = (x_1, x_2)$), and $d(\mathbf{x}, A)$ is the Euclidean distance from $\mathbf{x}$ to A.

When all polygons are the same and they are not too close, all points inside the polygons (including the sides) are Pareto optimal. Pareto optimal solutions in a polygon are overlapping with those in another polygon in the objective space.

As a two-dimensional decision space, we use $[0, 100] \times [0, 100]$ in all test problems in this paper. In Fig. 2 and Fig. 3, we show other test problems. While four rectangles in Fig. 2 are the same, Fig. 3 has two different trapezoids. As a result, a part of the inside of each trapezoid is not Pareto optimal. In each trapezoid, the shaded region is Pareto optimal. The shaded region in one trapezoid is not overlapping with the shaded region of the other trapezoid in the objective space except for (75, 83.125) and (25, 16.875). We examined the Pareto optimality of each of the 2001×2001 points (x_1 = 0.00, 0.05, 0.10, ..., 100.00; x_2 = 0.00, 0.05, 0.10, ..., 100.00) in the decision space $[0, 100] \times [0, 100]$.

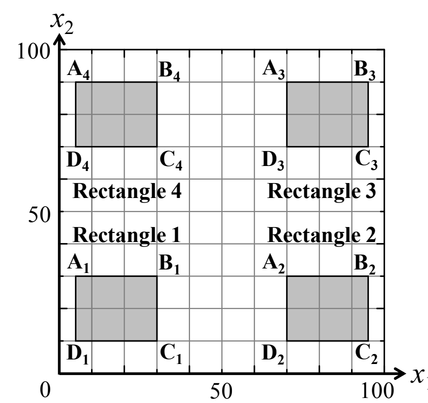

Figure 2. A polygon-based four-objective test problem.

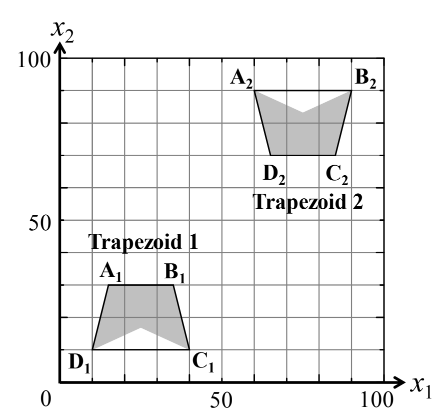

Figure 3. A four-objective problem with different trapezoids.

3. OUR MAP-BASED TEST PROBLEM

In Fig. 4, we show our map-based test problem generated from an actual real-world map. Our test problem includes six elementary schools (red circles), three junior-high schools (blue circles), 13 convenience stores (green circles), and three railway stations (purple circles). Four objectives to be minimized are defined using the Euclidean distance from a solution $\mathbf{x}$ in the decision space (i.e., a point in the map) as follows:

$f_1(\mathbf{x})$: Distance to the nearest elementary school (red circle),
$f_2(\mathbf{x})$: Distance to the nearest junior-high school (blue circle),
$f_3(\mathbf{x})$: Distance to the nearest convenience store (green circle),
$f_4(\mathbf{x})$: Distance to the nearest railway station (purple circle).

In Fig. 5, we show the Pareto optimal regions of our test problem. Our test problem has three disconnected Pareto optimal regions. As in Fig. 3, we examined the Pareto optimality of each of the 2001×2001 points (x_1 = 0.00, 0.05, 0.10, ..., 100.00; x_2 = 0.00, 0.05, 0.10, ..., 100.00) in the decision space $[0, 100] \times [0, 100]$ to depict the Pareto optimal regions in Fig. 5.

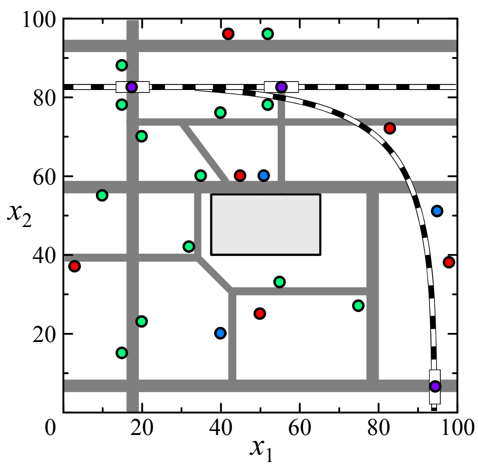

Figure 4. Our map-based four-objective test problem with six elementary schools (red circles), three junior-high schools (blue circles), 13 convenience stores (green circles), and three railway stations (purple circles).

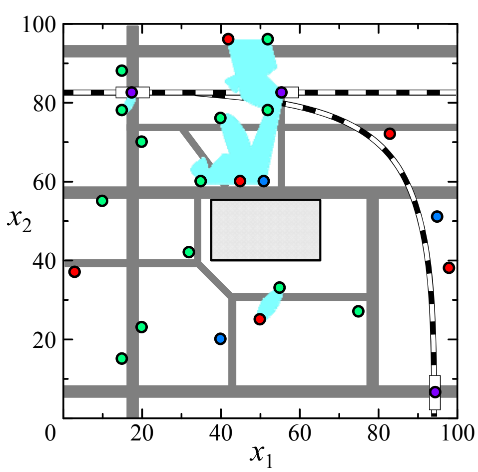

Figure 5. Pareto regions of our map-based test problem.

In Fig. 4, the location of each school (store, station) is specified as follows according to the actual real-world map:

Elementary schools: (3, 37), (42, 96), (45, 60), (50, 25), (83, 72), (98, 38),
Junior-high schools: (40, 20), (51, 60), (95, 51),
Convenience stores: (10, 55), (15, 15), (15, 78), (15, 88), (20, 23), (20, 70), (32, 42), (35, 60), (40, 76), (52, 78), (52, 96), (55, 33), (75, 27),
Railway stations: (17.5, 82.5), (55.5, 82.5), (94.5, 6.5).

4. EXPERIMENTAL RESULTS

In this section, we examine the behavior of EMO algorithms by applying them to the polygon-based test problems in Section 2 and our map-based test problem in Section 3.

4.1 Algorithms and Parameter Specifications

We applied NSGA-II, SPEA2, MOEA/D and SMS-EMOA to each test problem 100 times using the following specifications:

Total number of examined solutions: 20,000,
Initial population: Generated by random real numbers in [0, 100],
Population size: 200 (NSGA-II, SPEA2, and SMS-EMOA),
210 (MOEA/D for the three-objective problems),
220 (MOEA/D for the four-objective problems),
Crossover probability: 1.0 (SBX with $\eta_c = 15$),
Mutation probability: 0.5 (Polynomial mutation with $\eta_m = 20$),
Reference point in MOEA/D:
Minimum value of each objective in the current population,
Reference point in SMS-EMOA: 1.1 ×
Maximum value of each objective in the current population,
Neighborhood size in MOEA/D: 10% of the population size.

MOEA/D was implemented with no archive population using the Tchebycheff (Chebyshev) function. In MOEA/D, the population size is the same as the number of weight vectors. Due to the combinatorial nature of the number of uniformly distributed weight vectors, the population size cannot be arbitrarily specified in MOEA/D (for details, see Zhang and Li [21]). We used the closest integer to 200 among the possible values as the population size for MOEA/D (i.e., as the number of uniformly distributed weight vectors in MOEA/D). The same termination condition (i.e., 20,000 solution examinations) was used in all algorithms.

4.2 Performance Evaluation by Hypervolume

Each EMO algorithm was applied to each test problem 100 times. The average value of the hypervolume was calculated over 100 runs. The standard deviation was also calculated. In the hypervolume calculation, a reference point for each test problem was specified as "$\alpha \times$ (the maximum value of each objective in the true Pareto front)". When $\alpha = 1.1$, our reference point specification is the same as in SMS-EMOA. We examined various values of α: $\alpha = 1.0$, 1.1, 2.0 and 3.0. We also examined other two specifications of the reference point: (200, 200, 200, 200) and (400, 400, 400, 400). When the reference point is far from the Pareto front, extreme solutions around the edges of the Pareto front have large effects on the hypervolume calculation. When the reference point is very close to the Pareto front, solutions around the center region of the Pareto front have large effects on the hypervolume calculation.

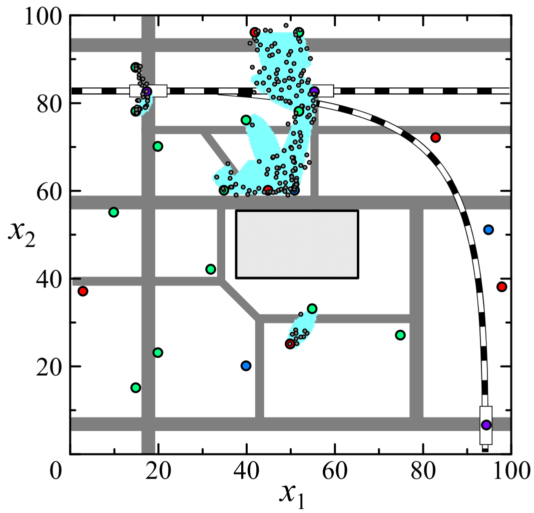

Figure 6. Obtained solutions by a single run of NSGA-II.

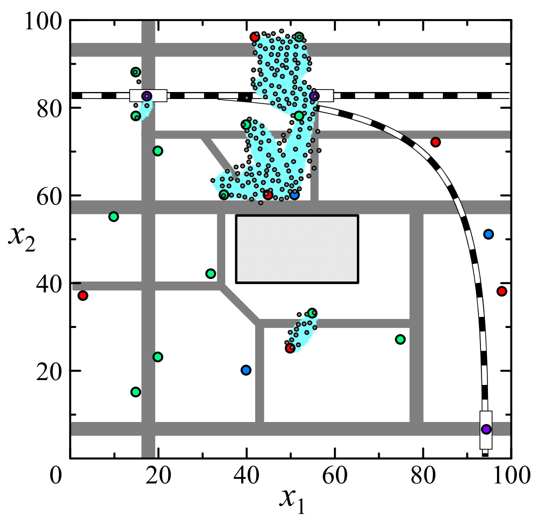

Figure 7. Obtained solutions by a single run of SPEA2.

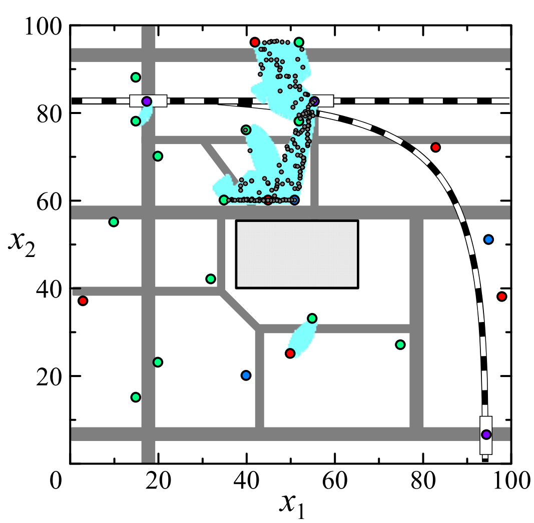

Figure 8. Obtained solutions by a single run of MOEA/D.

In Figs. 6-9, we show an obtained solution set by a single run of each EMO algorithm. From visual comparison among Figs. 6-9, we can see that the best results with respect to decision space diversity were obtained by SPEA2 in Fig. 7. In Table 1, we show the hypervolume of the solution set in each figure. The smallest value (i.e., the worst result) for each reference point is highlighted in boldface in Table 1. Whereas Fig. 7 by SPEA2 looks very good, the worst results in Table 1 were obtained by SPEA2 in many cases. To examine why the solution set in Fig. 7 does not have a high hypervolume value, we calculated the hypervolume of each solution set after including the green, red and blue circles around $30 < x_1 < 52$ and $x_2 = 60$. These three points were added to each solution set in Figs. 6-9. Experimental results are shown in Table 2. By including the three points, the hypervolume of the solution set in Fig. 7 was clearly improved in Table 2 from Table 1.

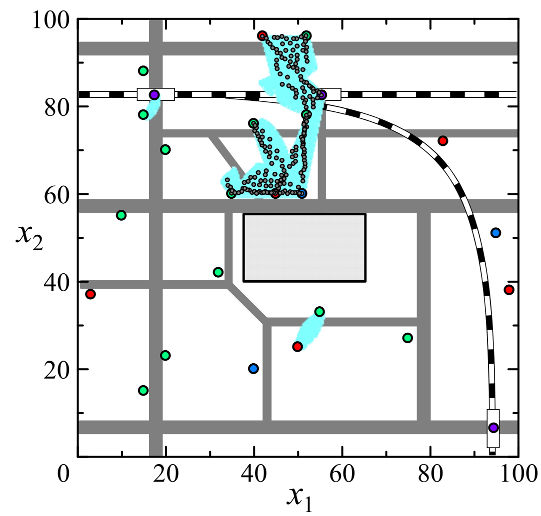

Figure 9. Obtained solutions by a single run of SMS-EMOA.

Table 1. Hypervolume of each solution set in Figs. 6-9. The smallest value for each reference point is highlighted by bold.

Reference Point	NSGA-II Figure 6	SPEA2 Figure 7	MOEA/D Figure 8	SMS-EMOA Figure 9
$\alpha=1.0$	**5.799E+05**	5.801E+05	5.873E+05	6.048E+05
$\alpha=1.1$	9.542E+05	**9.518E+05**	9.625E+05	9.856E+05
$\alpha=2.0$	1.479E+07	**1.467E+07**	1.478E+07	1.490E+07
$\alpha=3.0$	8.107E+07	**8.051E+07**	8.096E+07	8.131E+07
(200, ...)	1.571E+09	**1.564E+09**	1.571E+09	1.572E+09
(400, ...)	2.548E+10	**2.541E+10**	2.547E+10	2.548E+10

Table 2. Hypervolume of each solution set in Figs. 6-9 after the three points are included.

Reference Point	NSGA-II Figure 6	SPEA2 Figure 7	MOEA/D Figure 8	SMS-EMOA Figure 9
$\alpha=1.0$	**5.824E+05**	5.857E+05	5.933E+05	6.055E+05
$\alpha=1.1$	**9.579E+05**	9.617E+05	9.716E+05	9.867E+05
$\alpha=2.0$	**1.482E+07**	1.483E+07	1.485E+07	1.491E+07
$\alpha=3.0$	**8.118E+07**	8.120E+07	8.123E+07	8.137E+07
(200, ...)	**1.572E+09**	**1.572E+09**	**1.572E+09**	1.573E+09
(400, ...)	**2.548E+10**	2.549E+10	**2.548E+10**	2.549E+10

In Fig. 10, we show obtained solutions around the added three points. Each plot in Fig. 10 is the same as a small part of each figure in Figs. 6-9. From Fig. 10, we can see that SPEA2 found no solutions on the blue circle whereas the other algorithms found solutions on the blue circle. Those points on the blue circle in Fig. 10 (a), (c) and (d) are non-dominated solutions with the best value for the second objective (since the distance to the junior-high school is zero). That is, only SPEA2 did not find extreme solutions with the best value of the second objective. As a result, the hypervolume of the solution set in Fig. 7 by SPEA2 is not high while decision space diversity in Fig. 7 looks very good. In Fig. 10 (c), we can see that no solution was obtained by MOEA/D around the green circle. That is, MOEA/D did not find another extreme solution. This may be the reason why high hypervolume values were not obtained in Table 1 for the solution set in Fig. 8 (and also the reason for the improvement from Table 1 to Table 2).

In Table 3, we show the average hypervolume value over 100 runs of each algorithm together with the standard deviation in parentheses. Except for the case of $\alpha = 1.0$ (i.e., when the reference point was very close to the Pareto front), the worst results were obtained by SPEA2 for all the other cases. As shown in Fig. 7, SPEA2 found solution sets with good decision space diversity. However, SPEA2 was not highly evaluated in Table 3. The best results in Table 3 were obtained by SMS-EMOA. However, the decision space diversity in Fig. 9 is not so good.

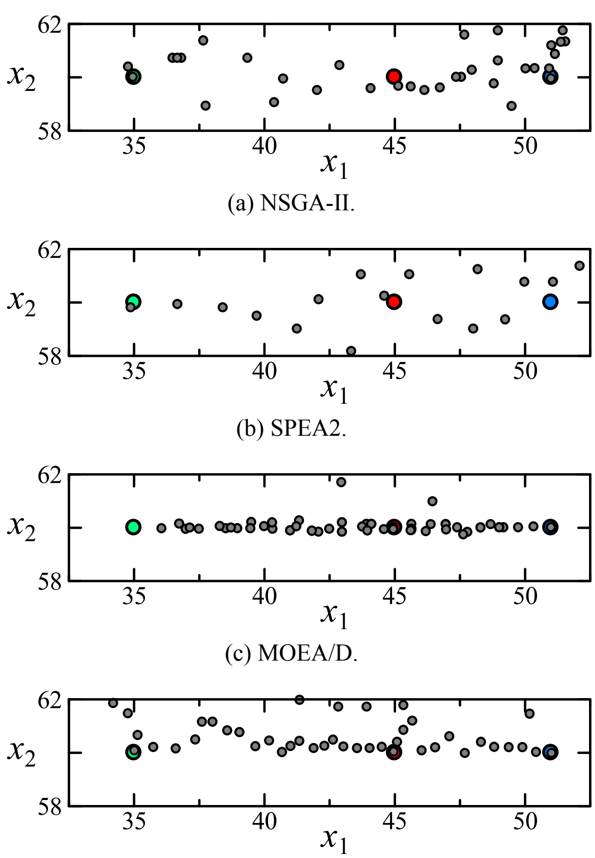

(a) NSGA-II.

(b) SPEA2.

(c) MOEA/D.

(d) SMS-EMOA.

Figure 10. Obtained solutions around the added three points. Only a small part of each figure in Figs. 6-9 is shown.

Table 3. Average hypervolume over 100 runs of each EMO algorithm. Standard deviation is shown in parentheses.

Reference Point	NSGA-II	SPEA2	MOEA/D	SMS-EMOA
$\alpha = 1.0$	**5.797E+05** (5.021E+03)	5.806E+05 (3.234E+03)	5.870E+05 (3.497E+03)	6.049E+05 (4.489E+02)
$\alpha = 1.1$	9.542E+05 (6.904E+03)	**9.518E+05** (4.733E+03)	9.625E+05 (4.792E+03)	9.856E+05 (6.821E+02)
$\alpha = 2.0$	1.479E+07 (3.608E+04)	**1.466E+07** (4.490E+04)	1.478E+07 (3.268E+04)	1.478E+07 (3.268E+04)
$\alpha = 3.0$	8.106E+07 (9.725E+04)	**8.046E+07** (1.921E+05)	8.094E+07 (1.198E+05)	8.129E+07 (3.449E+04)
(200, ...)	1.571E+09 (5.765E+05)	**1.564E+09** (2.398E+06)	1.570E+09 (1.288E+06)	1.572E+09 (5.233E+05)
(400, ...)	2.548E+10 (3.477E+06)	**2.541E+10** (2.162E+07)	2.546E+10 (1.166E+07)	2.548E+10 (4.742E+06)

Hypervolume has been frequently used in indicator-based EMO algorithms [2], [20], [22], [23]. Its property has also been actively studied [1], [7], [19]. Our experimental results in this section suggest that the relation between the hypervolume and the decision space diversity will be an interesting research issue.

4.3 Examination of Decision Space Diversity

As shown in Figs. 5-9, our test problem has three disconnected Pareto optimal regions in the decision space. The smallest one is around the railway station in the top-left corner of the decision space. The second smallest one is around the center of the decision space. After each run of each EMO algorithm, we counted the number of obtained solutions in each Pareto optimal region. Experimental results are summarized in Fig. 11 for the smallest Pareto optimal region and Fig. 12 for the second smallest Pareto optimal region. The horizontal axis of these figures shows the number of solutions in each Pareto optimal region while the vertical axis is the number of runs from which a particular numbers of non-dominated solutions were obtained. In Fig. 11 and Fig. 12, 100 runs of SMS-EMOA found no solutions in these small Pareto optimal regions. MOEA/D found no solutions in each small Pareto optimal region for about 90 runs.

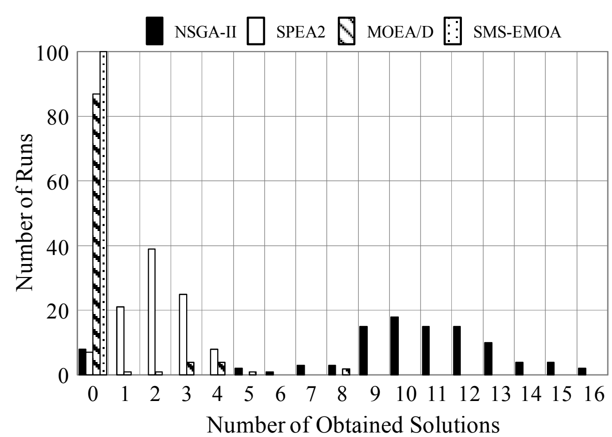

Figure 11. Number of obtained solutions in the smallest Pareto region of our test problem.

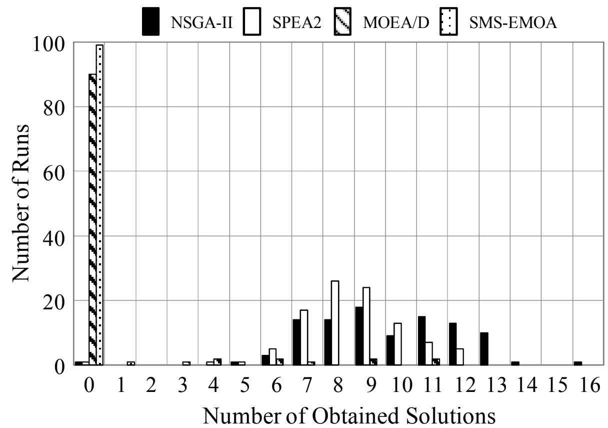

Figure 12. Number of obtained solutions in the second smallest Pareto region of our test problem.

From Fig. 11 and Fig. 12, we can also see that NSGA-II found at least four solutions in each of the small Pareto optimal regions in about 90 runs. SPEA2 found at least one solution in the smallest Pareto optimal region in about 90 runs in Fig. 11 and in the second smallest Pareto optimal region in almost all runs in Fig. 12.

For comparison, we also performed the same computational experiments on the three test problems in Section 2. In Fig. 13, we show obtained solutions by a single run of each EMO algorithm on the triangle-based three-objective test problem with the equivalent Pareto optimal regions. Since the four Pareto optimal regions in Fig. 13 are exactly the same in the objective space, it is very difficult for EMO algorithms to find solutions uniformly distributed over the four triangles.

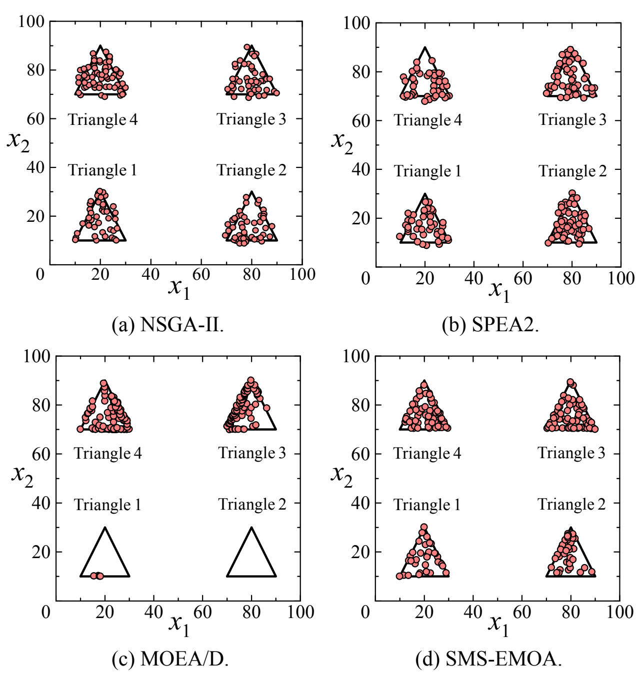

Figure 13. Obtained solutions by a single run of each algorithm on the triangle-based test problem.

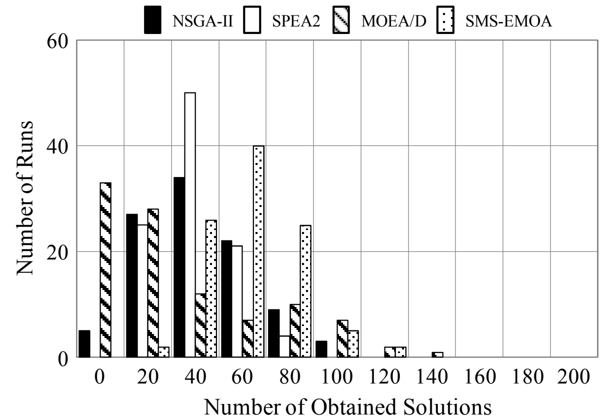

Figure 14. Number of obtained solutions in Triangle 1.

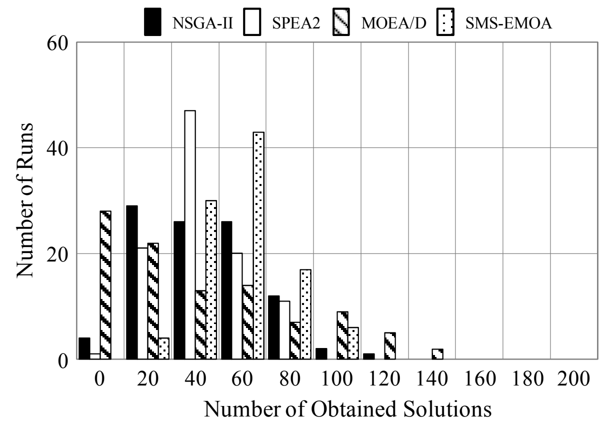

Figure 15. Number of obtained solutions in Triangle 2.

In Fig. 14 and Fig. 15, we show the number of obtained solutions in Triangle 1 and Triangle 2, respectively. The number of obtained solutions along the horizontal axis is discretized into 11 intervals as [0, 0], [1, 20], [21, 40], ..., [181, 200]. Since we have the four triangles and a population of 200 individuals, we may have 50 solutions in each triangle in an ideal situation. In Fig. 14 and Fig. 15, MOEA/D and NSGA-II found no solutions in a particular triangle in about 30 runs and 5 runs, respectively. SMS-EMOA found at least one solution in each of Triangle 1 and Triangle 2 in their 100 runs.

From Figs. 13-15, we can see that good decision space diversity was obtained by SMS-EMOA for the triangle-based test problem. This observation clearly contrasts with the behavior of SMS-EMOA in Fig. 11 and Fig. 12 where no solutions were found in the two disconnected small Pareto optimal regions by its 100 runs.

For comparison, we also report experimental results of a single run of each algorithm on the rectangle-based test problem in Fig. 16. The number of obtained solutions in Rectangle 1 is shown in Fig. 17. From experimental results in Fig. 16 and Fig. 17, we can see that good decision space diversity was obtained by SMS-EMOA. We obtained the same observation from Figs. 13-15 for the triangle-based test problem and a totally opposite observation from Fig. 11 and Fig. 12 for our map-based test problem.

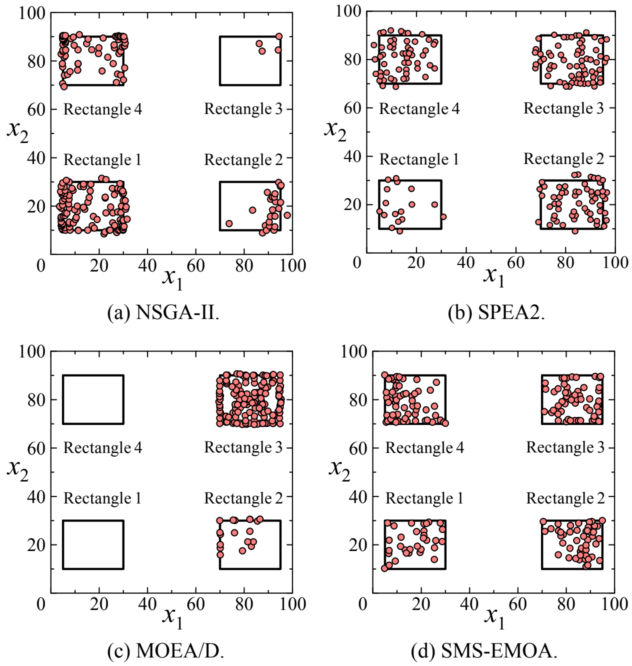

Figure 16. Obtained solutions by a single run of each algorithm on the rectangle-based test problem.

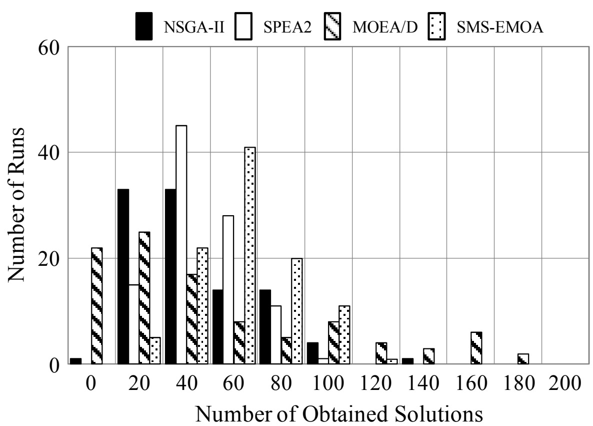

Figure 17. Number of obtained solutions in Rectangle 1.

In Fig. 18, we show experimental results of a single run of each algorithm on the trapezoid-based test problem. The two Pareto optimal regions in this problem are not equivalent. Thus the diversity maintenance in each EMO algorithm in the objective space should have some effect on the decision space diversity. The number of obtained solutions in Trapezoid 1 is shown in Fig. 19. From Fig. 19, we can see that 81-120 solutions were always obtained by SMS-EMOA. We can also see from Fig. 19 that 41-100 solutions were almost always obtained by NSGA-II. As in the case of the triangle-based and rectangle-based test problems, good decision space diversity was obtained by SMS-EMOA for the trapezoid-based test problem in Fig. 18 and Fig. 19. This observation clearly contrasts to the behavior of SMS-EMOA on our map-based test problem in Fig. 11 and Fig. 12.

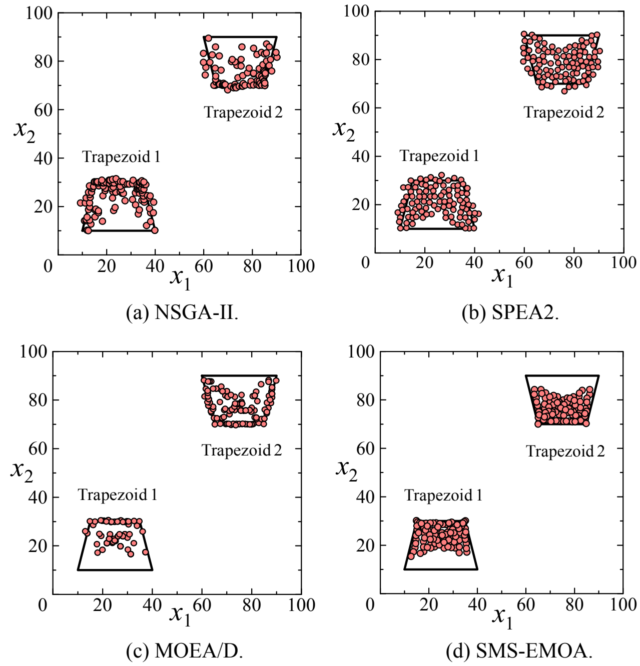

Figure 18. Obtained solutions by a single run of each algorithm on the trapezoid-based test problem.

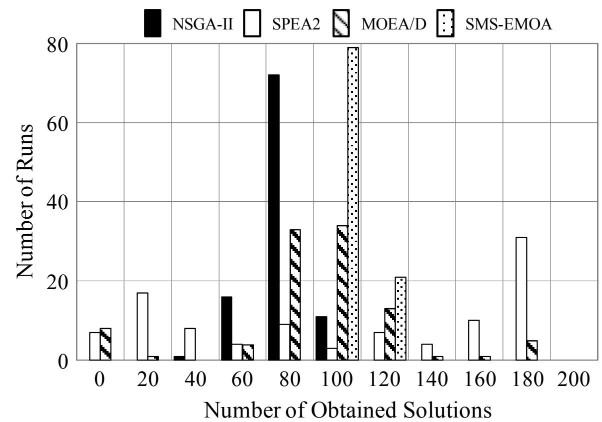

Figure 19. Number of obtained solutions in Trapezoid 1.

5. CONCLUSIONS

In this paper, we first generated a distance minimization problem from an actual real-world map. Our map-based test problem has three disconnected Pareto optimal regions in a two-dimensional decision space. Next we applied NSGA-II, SPEA2, MOEA/D and SMS-EMOA to our test problem. We observed in computational experiments that good decision space diversity was obtained by SPEA2. However, the hypervolume of a solution set with good decision space diversity by SPEA2 was the worst among the four EMO algorithms. Further examination showed that some extreme solutions with the best value of a single objective were not obtained by SPEA2. This may be the reason why the hypervolume of solution sets by SPEA2 for our test problem was the worst among the examined four EMO algorithms. We also examined the decision space diversity using other test problems with multiple polygons. An interesting observation is that SMS-EMOA showed the best diversity maintenance ability in the decision space for the three polygon-based test problems while it showed the worst decision space diversity for our map-based test problem. It is left for future studies to examine why totally different results were obtained by SMS-EMOA.

6. REFERENCES

[1] Auger, A., Bader, J., Brockhoff, D., and Zitzler, E. Theory of the hypervolume indicator: Optimal μ-distributions and the choice of the reference point. *Proc. of Foundations of Genetic Algorithm X* (2009) 87-102.

[2] Beume, N., Naujoks, B., and Emmerich, M. SMS-EMOA: multiobjective selection based on dominated hypervolume. *European Journal of Operational Research* 180, 3 (2007) 1653-1669.

[3] Coello, C. A. C. and Lamont, G. B. *Applications of Multi-Objective Evolutionary Algorithms*. World Scientific, Singapore (2004).

[4] Coello, C. A. C., van Veldhuizen, D. A., and Lamont, G. B. *Evolutionary Algorithms for Solving Multi-Objective Problems*. Kluwer, Boston (2002).

[5] Deb, K. *Multi-Objective Optimization Using Evolutionary Algorithms*. John Wiley & Sons, Chichester (2001).

[6] Deb, K., Pratap, A., Agarwal, S., and Meyarivan, T. A fast and elitist multi-objective genetic algorithm: NSGA-II. *IEEE Trans. on Evolutionary Computation* 6, 2 (2002) 182-197.

[7] Friedrich, T., Horoba, C., and Neumann, F. Multiplicative approximations and the hypervolume indicator. *Proc. of 2009 Genetic and Evolutionary Computation Conference* (2009) 571-578.

[8] Hughes, E. J. Evolutionary many-objective optimization: Many once or one many?. *Proc. of 2005 IEEE Congress on Evolutionary Computation* (2005) 222-227.

[9] Ishibuchi, H., Hitotsuyanagi, Y., and Nojima, Y. Many-objective test problems to visually examine the behavior of multi-objective evolution in a decision space. *Lecture Notes in Computer Science, Vol. 6239: PPSN XI*, Springer, Berlin (2010) 91-100.

[10] Ishibuchi, H., Tsukamoto, N., Hitotsuyanagi, Y., and Nojima, Y. Effectiveness of scalability improvement attempts on the performance of NSGA-II for many-objective problems. *Proc. of 2008 Genetic and Evolutionary Computation Conference* (2008) 649-656.

[11] Khara, V., Yao, X., and Deb, K. Performance scaling of multi-objective evolutionary algorithms. *Lecture Notes in Computer Science, vol. 2632: Evolutionary Multi-Criterion Optimization - EMO 2003*, Springer, Berlin (2004) 367-390.

[12] Köppen, M. and Yoshida, K. Substitute distance assignments in NSGA-II for handling many-objective optimization problems. *Lecture Notes in Computer Science, vol. 4403: Evolutionary Multi-Criterion Optimization - EMO 2007*, Springer, Berlin (2007) 727-741.

[13] Kramer, O. and Danielsiek, H. DBSCAN-based multi-objective niching to approximate equivalent Pareto-subsets. *Proc. of 2010 Genetic and Evolutionary Computation Conference* (2010) 503-510.

[14] Purshouse, R. C. and Fleming, P. J. On the evolutionary optimization of many conflicting objectives. *IEEE Trans. on Evolutionary Computation* 11, 6 (2007) 770-784.

[15] Rudolph, G., Naujoks, B., and Preuss, M. Capabilities of EMOA to detect and preserve equivalent Pareto subsets. *Lecture Notes in Computer Science, vol. 4403: Evolutionary Multi-Criterion Optimization - EMO 2007*, Springer, Berlin (2007) 36-50.

[16] Schutze, O., Lara, A., and Coello, C. A. C. On the influence of the number of objectives on the hardness of a multiobjective optimization problem. *IEEE Trans. on Evolutionary Computation* (to appear: online available from IEEE Xplore).

[17] Singh, H., Isaacs, A., Ray, T., and Smith, W. A study on the performance of substitute distance based approaches for evolutionary many-objective optimization. *Lecture Notes in Computer Science, Vol. 5361: SEAL 2008*, Springer, Berlin, (2008) 411-420.

[18] Tan, K. C., Khor, E. F., and Lee, T. H. *Multiobjective Evolutionary Algorithms and Applications*, Springer, Berlin (2005).

[19] Ulrich, T., Bader, J., and Zitzler, E. Integrating decision space diversity into hypervolume-based multiobjective search. *Proc. of 2010 Genetic and Evolutionary Computation Conference* (2010) 455-462.

[20] Wagner, T., Beume, N., and Naujoks, B. Pareto-, aggregation-, and indicator-based methods in many-objective optimization. *Lecture Notes in Computer Science, vol. 4403: Evolutionary Multi-Criterion Optimization - EMO 2007*, Springer, Berlin (2007) 742-756.

[21] Zhang, Q. and Li, H. MOEA/D: A multiobjective evolutionary algorithm based on decomposition. *IEEE Trans. on Evolutionary Computation* 11, 6 (2007) 712-731.

[22] Zitzler, E., Brockhoff, D., and Thiele, L. The hypervolume indicator revisited: On the design of Pareto-compliant indicators via weighted integration. *Lecture Notes in Computer Science, vol. 4403: Evolutionary Multi-Criterion Optimization - EMO 2007*, Springer, Berlin (2007) 862-876.

[23] Zitzler, E. and Künzli, S. Indicator-based selection in multiobjective search. *Lecture Notes in Computer Science 3242: Parallel Problem Solving from Nature - PPSN VIII*, Springer, Berlin (2004) 832-842.

[24] Zitzler, E., Laumanns, M., and Thiele, L. SPEA2: Improving the strength Pareto evolutionary algorithm," *TIK-Report 103*, Computer Engineering and Networks Laboratory (TIK), ETH, Zurich (2001).

[25] Zitzler, E. and Thiele, L. Multi-objective evolutionary algorithms: A comparative case study and the strength Pareto approach. *IEEE Trans. on Evolutionary Computation* 3, 4 (1999) 257-271.